Electronic Supporting Information (ESI)

Solvent dependent ESIPT based probe for optical recognition of Zr(IV) and Zn(II)

Tandrim Shyam[a], Subhasis Ghosh,[a] Sangita Maji[a], Prosenjit Mandal[a] and Debasis Das*[a]
[a]Department of Chemistry, The University of Burdwan, Burdwan, West Bengal, India

1. EXPERIMENTAL

Materials

All the experimental procedures have been performed under aerobic condition. High-purity PBS, 2, 6-diformyl-4-methyl phenol (**DFP**) and 1-ethynylcyclohexylamine were purchased from SigmaAldrich (India). $ZrO(NO_3)_2$ and $Zn(OAc)_2$ were purchased from Merck (India). The solvents used were of spectroscopic grade. Other chemicals were of analytical reagent grade and used without further purification. Mili-Q Milipore 18.2 MΩcm^{-1}water was used whenever required.

Physical measurements

Physical measurements have been carried out using the following instruments. A Shimadzu Multi Spec 2450 spectrophotometer was used for recording UV-Vis. spectra. FTIR spectra were recorded on a Shimadzu FTIR (model IR Prestige 21 CE) spectrophotometer. High resolution mass spectra are recorded using Xevo G2S/Q-Toff. micro^{TM} spectrometer. ^{1}HNMR spectra are recorded in DMSO-d_6 and $CDCl_3$ using Bruker Advance 400 (400 MHz) instrument. The steady state emission and excitation spectra were recorded with a Hitachi F-7100 spectrofluorimeter. A Systronics digital pH meter (model 335) was used for pH measurement. Single crystal X-ray diffraction data were collected on a Bruker X8 APEX-II CCD diffractometer at 100(2) K using graphite-monochromated Mo-Kα radiation (0.71073Å) at 150K. Data were processed and corrected for Lorentz and polarization absorption effects. Crystal structures were solved by standard direct methods using SHELXS43 and refined by full-matrix leastsquares with SHELXL44 and OLEX2 soft ware.

Spectroscopic and crystallographic characterization

A. 2, 6-Bis-[(1-ethynyl-cyclohexylimino)-methyl]-4-methyl-phenol (DEC)

DEC has molecular formula $C_{25}H_{30}N_2O$ (MW, 374.52). Anal. found (%): C, 80.14; H, 8.06 and N, 7.47; Calcd. (%), C, 80.17; H, 8.07 and N, 7.48. ESI-MS (*m/z*): [M-H] $^+$, 373.21[Figure S1a]. FTIR (KBr, cm^{-1}): 3284, *ν*(C–H, stretch, alkyne); 3214, *ν*(O–H, stretch); 2933, *ν*(C–H, sp^2); 1627, *ν*(C=N, stretch); 1598, *ν*(C=C, stretch); 1450, *ν*(C–H, bending), 1349, *ν*(C–O, stretch); and 1252, *ν*(C–N, aromatic). [Figure S1b] ^{1}H NMR ($CDCl_3$, 500 MHz, *J*, Hz, δ ppm, reference peak

7.26 ppm) [Fig. S1c and S1d]: 10.914 (1H, s); 8.872 (2H, s); 7.739 (2H,s); 2.746 (3H, s), 2.382 (2H, s) and 1.238-2.234 (10H, m). [Figure S1c] The structure is also confirmed by SC-XRD analysis.

Single crystal X-ray diffraction analysis of DEC

DEC is characterized by spectroscopic techniques and it's stereo-chemical structure is confirmed by single crystal X-ray diffraction analysis. The molecular view and atom labeling scheme and packing patterns are shown in Figure S1d. The crystallographic data and refinement parameters are presented in Table S1 while selected bond length and angles are listed in Table S2.

DEC has triclinic space group P -1 (CCDC1979508): a, 9.602(7) (Å); b, 9.726(8) (Å), c, 13.486(12) (Å); α (°), 68.55(3); β (°), 73.114(19) (3); γ (°), 68.923(18); volume (Å^3), 1075.4(16); Z = 2 (Table S1). DEC exists in enol form in solid state. The bond lengths N003 C19, 1.2650(17) (Å); and N002 C11, 1.2563(16)(Å) indicate the C-N double bond character while N003 C23, 1.4799(15)(Å) andN002 C5, 1.4724(18)(Å) indicate the C-N single bond character. On the other hand, O001 C18, 1.3434(16)(Å) shows single bonded character of C-O in phenol moiety. The structure is also stabilized by intra-molecular H-bonding. The bond angles C19 N003 C23, 121.31(11) (°) and C11 N002 C5, 121.59(10)(°) indicate the sp^2 nature of N003 and N002 centers.

B. DEC-Zr(IV) adduct (Ad1)

Molecular formula: $C_{50}H_{58}N_6O_8Zr$. Anal. found (%): C, 62.38; H, 6.07 and N, 6.49. calcd. (%), C, 62.41; H, 6.08 and N, 6.53 O. ESI-MS (*m/z*): [**Ad1**+H] $^+$, 962.27 [Figure S2a]. FTIR (KBr, cm^{-1}): 3294, *ν*(C–H, str., alkyne); 3078, *ν*(C–H, str., sp^2); 3037, *ν*(C–H, str., sp^2); 2928, *ν*(C–H, str., sp^3); 2887, *ν*(C–H, str., sp^3); 1688, *ν*(C=N, stretch); 1600, *ν*(C=C, stretch); 1478, *ν*(C–H, bend.); 1280, *ν*(C–N, str.) and 1192, *ν*(C–O, str.) [Figure S3a].

C. DEC-Zn(II) adduct (Ad2)

Molecular formula: $C_{27}H_{32}N_2O_3Zn$. Anal. found (%): C, 65.09; H, 6.88; N, 5.33 and O, 8.65; calcd. (%), C, 65.13; H, 6.90 and N, 5.33. ESI-MS (*m/z*): [**Ad2**+H] $^+$, 498.16 [Figure S2b]. FTIR (KBr, cm^{-1}): 3288, *ν*(C–H, str., alkyne); 3076, *ν*(C–H, str., sp^2); 2883, *ν*(C–H, str., sp^3); 2794, *ν*(C–H, str., sp^3); 1687, *ν*(C=N, stretch); 1586, *ν*(C=C, stretch); 1507, *ν*(C–H, bend.); 1434, *ν*(C–H, bend.); 1203, *ν*(C–N, str.) and 1171, *ν*(C–O, stretch) [Figure S3b].

General method of UV-Vis. and fluorescence titration

For absorption and emission spectroscopic data, cells having 1 cm path length were used. Stock solutions of DEC, $Zr(NO_3)_4$ and $Zn(NO_3)_2$ were prepared both in EtOH-water (1:4, v/v) and DMSO-water (1:5, v/v). Their working solutions were prepared from respective stock solutions *via* appropriate dilution. Fluorescence measurements were performed using 5 nm × 5 nm slit

width, where the excitation wavelengths in EtOH-water and DMSO-water were 380 nm and 350 nm respectively. All spectra were recorded at room temperature.

Job's plot from fluorescence experiment

The sets of solutions containing **DEC** and analyte [Zr(IV) and Zn(II)] are so prepared that the total concentration of **DEC** and analyte remain constant (5 μM) in all the sets. The mole fraction (X) of analyte is varied from 0.1 to 0.9 for all sets. The emission intensities at 508 nm for Zr(IV) (λ_{ex} = 370 nm) and 475 nm for Zn(II) (λ_{ex}= 350 nm) are plotted as a function of mole fraction of Zr(IV) and Zn(II) respectively. **DEC** forms 2:1 (mole ratio) adduct with Zr(IV) and 1:1 (mole ratio) adduct with Zn(II). This is also confirmed from their respective mass spectra.

Determination of binding constant

The binding constants between **DEC** and two analyte, Zr(IV) and Zn(II) are determined employing modified Benesi-Hildebrand equation[1]: $\mathbf{(F_{max}–F_0)/ (F_x–F_0) = 1+ (1/K) (1/[C]^n)}$ where, F_{max}, F_0 and F_x are emission intensities for **DEC** in presence of analyte at saturation, in absence of analyte and at any intermediate analyte concentrations respectively. The plots of $(F_{max}–F_0)/ (F_x–F_0)$ *vs.* $[C]^{-1}$ (here, n = 1.0) generate the binding constants from the slope while [C] is molar concentration of analyte.

Determination of detection limit

The detection limit (**DL**) is estimated using the following equation[2]:

$$DL = \frac{3\sigma}{S}$$

σ is the standard deviation of the blank solution, **S** is the slope of the calibration curve.
For determination of standard deviation, the emission intensity of **DEC** without any analyte was measured 10 times.[3]

Time correlated single photon counting (TCSPC) experiment

Fluorescence lifetime data of all compounds were measured with a Horiba Delta Flex^{tm} time correlated single photon counting (TCSPC) instrument. A laser operating γ_{max} = 403 nm with a repetition rate of 1 MHz is used as the excitation source. The width of the instrument function, which was limited by the FWHM of the excitation source, was 110ps. The lamp profile was recorded by placing a scatterer in place of the sample. The signal was collected at the magic angle of 54.7^o. The decay were deconvoluted using DAS-6 decay analysis software and acceptability of fits was judged by χ^2 criteria.
The relative contributions (α_n) to the fluorescence decay of the multi exponential decay were obtained using the following relation[7].

$$\alpha_n = \frac{B_n}{\sum_{i=1}^{n} B_i}$$

B_i is the pre-exponential factor of a single exponential decay. The average lifetime of the compound was calculated using the following relation:

$$\langle \tau \rangle = \frac{\sum_{i=1}^{n} \alpha_i t_i^2}{\sum_{i=1}^{n} \alpha_i t_i}$$

Determination of quantum yield

The fluorescence quantum yields are determined using naphthalene as reference having ϕ_R, 0.2 in MeOH[4]. The sample and the reference dye are excited at same wavelength (λ_{ex}, 380 nm for EtOH-water and λ_{ex}, 350 nm for DMSO-water media), maintaining nearly equal absorbance (0.1) and emission intensities. The area of the emission spectra are measured and the quantum yields are calculated following the equation[5], $\phi_S / \phi_R = [A_S/A_R] \times [(Abs)_R/(Abs)_S] \times [\eta_S^2/ \eta_R^2]$, where ϕ_S and ϕ_R are fluorescence quantum yields of the sample and reference respectively, A_S and A_R are area under the fluorescence spectra of the sample and the reference respectively, $(Abs)_S$ and $(Abs)_R$ are the corresponding optical densities of the sample and the reference solution at the wavelength of excitation; η_S and η_R are the refractive indices of the sample and reference, respectively[6].

The quantum yields of free **DEC** and [**DEC**-Zr(IV)]adduct (**Ad1**) in PBS buffer media (10 mM, pH 7.4) are 0.017 and 0.1432 respectively in EtOH-water media. On the other hand, the quantum yields of free **DEC** and [DEC-Zn(II)] adduct (**Ad2**) in PBS buffer media (10 mM, pH 7.4) are 0.0186 and 0.1512 respectively in DMSO-water media.

Table S1 Crystallographic data table for **DEC**

Molecule	**DEC**
CCDC	1979508
Empirical formula	C25H30N2O
Formula weight	374.51
Crystal system	Triclinic
Space group	P -1

Temperature	296K
Wavelength	0.71073
a/Å	9.602(7)
b/Å	9.726(8)
c/Å	13.486(12)
α/°	68.55(3)
β/°	73.114(19)
γ/°	68.923(18)
Volume/Å^3	1075.4(16)
Z	2
ρ_{calc} g/cm^3	1.157

Table S2 Selected bond lengths [Å] and angles [°] for **DEC**

ATOMS	**BOND LENGTH**	**ATOMS**	**BOND ANGLE**
O001 C18	1.3434(16)	C11 N002 C5	121.59(10)
N002 C11	1.2563(16)	C19 N003 C23	121.31(11)
N002 C5	1.4724(18)	O001 C18 C12	119.43(11)
N003 C19	1.2650(17)	O001 C18 C17	120.93(10)
N003 C23	1.4799(15)	C12 C18 C17	119.63(11)
C18 C12	1.3973(16)	N002 C5 C3	113.78(10)
C18 C17	1.4045(19)	N002 C5 C6	107.09(9)
C5 C3	1.4691(19)	C3 C5 C6	109.80(12)
C5 C6	1.531(2)	N002 C5 C10	106.71(11)
C5 C10	1.536(2)	C3 C5 C10	109.79(11)
C12 C13	1.3834(18)	C6 C5 C10	109.55(10)
C12 C11	1.4683(19)	C18 C12 C13	118.87(11)
C13 C15	1.3840(19)	C18 C12 C11	120.69(11)
C17 C16	1.3883(19)	C13 C12 C11	120.44(10)
C17 C19	1.4530(17)	C15 C13 C12	122.96(10)
C15 C16	1.3862(18)	N002 C11 C12	120.91(11)
C15 C14	1.497(2)	C16 C17 C18	118.99(10)
C23 C20	1.469(2)	C16 C17 C19	120.03(11)
C23 C29	1.532(2)	C18 C17 C19	120.94(11)
C23 C28	1.522(2)	C16 C15 C13	117.07(11)
C6 C7	1.523(2)	C16 C15 C14	121.99(12)
C3 C4	1.1675(19)	C13 C15 C14	120.93(11)
C10 C9	1.517(2)	C20 C23 N003	111.74(11)
C28 C22	1.521(2)	C20 C23 C29	110.35(11)
C29 C26	1.5272(19)	N003 C23 C29	108.19(11)
C20 C21	1.173(2)	C20 C23 C28	109.80(12)
C7 C8	1.513(2)	N003 C23 C28	107.30(10)
C26 C27	1.507(3)	C29 C23 C28	109.37(12)
C22 C27	1.510(3)	N003 C19 C17	122.12(12)
C9 C8	1.504(2)	C7 C6 C5	112.52(10)
		C4 C3 C5	179.58(16)

		C15 C16 C17	122.37(12)
		C9 C10 C5	112.25(11)
		C22 C28 C23	112.08(11)
		C23 C29 C26	111.31(12)
		C21 C20 C23	177.95(17)
		C27 C26 C29	110.59(12)
		C27 C22 C28	111.56(13)
		C8 C9 C10	111.09(12)
		C22 C27 C26	111.53(13)
		C9 C8 C7	110.77(12)

Table S3 Results from TD-DFT calculations on DEC

Compound	Electronic Transitions	Energy[a] (eV)	Wavelength (nm)	f[b]	Transitions involved
DEC	**$S_0 \rightarrow S_1$**	**3.6827 eV**	**336.66 nm**	**f=0.1589**	**HOMO→LUMO**
	$S_0 \rightarrow S_2$	**4.3617 eV**	**284.25 nm**	**f=0.0013**	**HOMO-1→LUMO HOMO-2→LUMO HOMO-2→LUMO+1**
	$S_0 \rightarrow S_3$	**4.6318 eV**	**267.68 nm**	**f=0.0241**	**HOMO-1→LUMO HOMO-1→LUMO+1 HOMO→LUMO+1**
Ad1	**$S_0 \rightarrow S_1$**	**1.5866 eV**	**781.47 nm**	**f=0.0049**	**HOMO-1→LUMO HOMO-1→LUMO+2**
	$S_0 \rightarrow S_2$	**1.7158 eV**	**722.62 nm**	**f=0.0049**	**HOMO→LUMO HOMO-2→LUMO**
	$S_0 \rightarrow S_3$	**1.7657 eV**	**702.19 nm**	**f=0.0101**	**HOMO→LUMO HOMO-2→LUMO**
Ad2	**$S_0 \rightarrow S_1$**	**2.4704 eV**	**501.89 nm**	**f=0.0010**	**HOMO→LUMO HOMO-1→LUMO**
	$S_0 \rightarrow S_2$	**3.1461 eV**	**394.08 nm**	**f=0.0831**	**HOMO→LUMO HOMO-1→LUMO**
	$S_0 \rightarrow S_3$	**3.3317 eV**	**372.14 nm**	**f=0.0090**	**HOMO→LUMO+1 HOMO-1→LUMO+1**

Comparison of sensing parameters of DEC with reported probes

Efficiency of **DEC** is compared with that of reported probes **(Table S4)**. It is noteworthy that fluorescence sensors of Zr(IV) is very rare. The **DEC** detectws Zr(IV) with good detection limit through turn on fluorescence as well as Zn(II) with good LOD. Easy synthesis, quick response and resonable LOD make DEC useful for practical application.

Table S4 Comparison of **DEC** with reported literature

Sl. No.	**System (probe)**	**Type**	**Limit of detection (LOD)**	**Ref.**
1	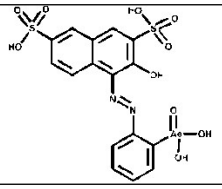	PVC membrane-based electrode sensor	6.0×10^{-7} mol L^{-1} [for Zr(IV)]	8
2	2-(Bis-(pyridin-2-ylmethyl)amino)ethan-1-ol and GO hybrid (GOP)	Turn-on fluorescence sensor	27 ng mL^{-1} [for Zr(IV)]	9
3	4-Chloro-N-(2,6-dimethylphenyl)-2-hydroxy-5-sulfamoylbenzamide (xipamide, XM)	Potentiometric sensor	1.0×10^{-6} mol L^{-1} [for Zr(IV)]	10
4	Gold cysteamine self-assembled monolayer by nitrilotriacetic acid	Electrochemical impedance spectroscopy	7.8×10^{-10} M [for Zr(IV)]	11
5	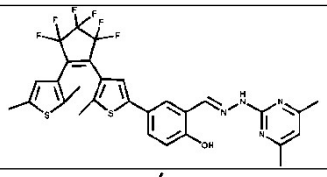	Turn-on fluorescence sensor	8.48 $C10^{-8}$ mol L^{-1} [for Zn(II)]	12
6	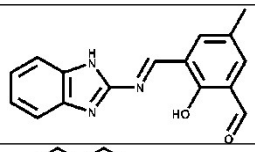	Turn-on fluorescence sensor	0.832 nM [for Zn(II)]	13
7	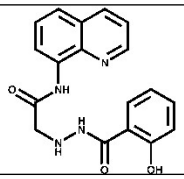	Turn-on fluorescence sensor	1.4×10^{-7} M [for Zn(II)]	14

8	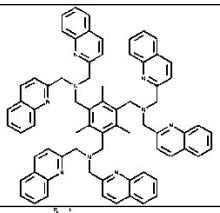	Turn-on fluorescence sensor	35.60 × 10^{-9} M and 29.45 × 10^{-8} M [for Zn(II)]	15
9	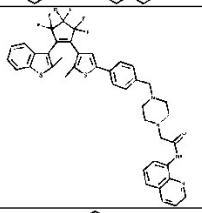	Turn-on fluorescence sensor	5.5 × 10^{-5} mol L^{-1} [for Zn(II)] 2.7 × 10^{-5} mol L^{-1} [For Cu(II)]	16
10	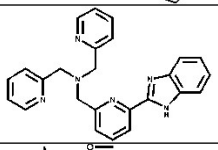	Turn-on fluorescence sensor	[for Zn(II)]	17
11	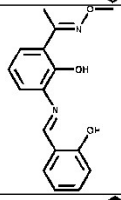	Turn-on fluorescence sensor	1.44 × 10^{-7} M [For Zn(II)]	18
12	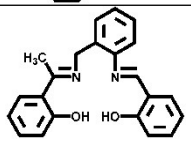	Turn-on fluorescence sensor	49 nM [for Al(III)] 35 nM [For Zn(II)]	19
13	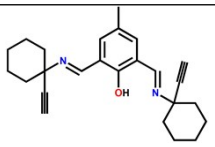 **DEC**	Turn-on fluorescence sensor	19.43 nM [for Zr(IV)] and 23.46 nM for Zn(II)]	Present report

Reference

1. H. A. Benesi and J. H. Hildebrand, *J. Am. Chem. Soc.*, 1949, **71**, 2703-2707
2. M. Zhu, M. Yuan, X. Liu, J Xu, J. Lv, C. Huang, H. Liu, Y. Li, S. Wang and D. Zhu, *Org. Lett.*, 2008, **10**, 1481-1484
3. S. Dey, R. Purkait, K. Pal, K. Jana and C. Sinha, *ACS Omega*, 2019, **4**, 8451-8464
4. W. H. Melhuish, *J. Phys. Chem*., 1961, **65**, 229-235
5. E. Austin and M. Gouterman, *Bioinorg. Chem*., 1978, **9**, 281-298
6. F. I. El-Dossoki, *J. Chin. Chem. Soc*., 2007, **54**, 1129-1137
7. S. Khanra, S. Ta, M. Ghosh, S. Chatterjee, P. Mukherjee and D. Das, *New J. Chem.*, 2020,**44**, 8477-8485
8. H. A. Arida, *Talanta*, 2008, **76**, 40–43
9. J. B. Asha and P. Suresh, *ACS Sustainable Chemistry & Engineering,* 2020, **8(38)**, 14301-14311
10. G. G. Mohameda, H. A. Mohameda and E. Y. Frag, *Microchemical Journal*, 2020, **157**, 105063
11. R. K. Shervedan and M. Bagherzadeh, *Sensors and Actuators B,* 2009, **139**, 657–664

12. X. Wu, Z. Zhang, H. Liu and S. Pu, *RSC Adv*., 2020, **10**, 15547-15553
13. S. Dey, A. Roy , G. P. Maiti, S. K. Mandal, P. Banerjee and P. Roy, *New J. Chem.*, 2016, **40**, 1365-1376
14. L. Gu, X. Wan, H. Liu, T. Liu and Y. Yao, *Anal. Methods*, 2014,**6**, 8460-8463
15. S. Sinha, B. Chowdhury, N. N. Adarsh and P. Ghosh, *Dalton Trans.*, 2018,**47**, 6819-6830
16. S. Xia, G. Liu and S. Pu, *J. Mater. Chem. C*, 2015,**3**, 4023-4029
17. Z. Liu, C. Zhang, Y. Li, Z. Wu, F. Qian, X.Yang, W. He, X. Gao and Z. Guo, *Org. Lett*., 2009, **11**, 795-798
18. W. K. Dong, S. F. Akogun, Y. Zhang, Y. X. Sun and X. Y. Dong, *Sensors and Actuators B*, 2017, **238**, 723–734
19. T. Shyam, M. Ghosh, S. Ghosh, and D. Das, *Chemistry Select,* 2023, **8**, e202204534

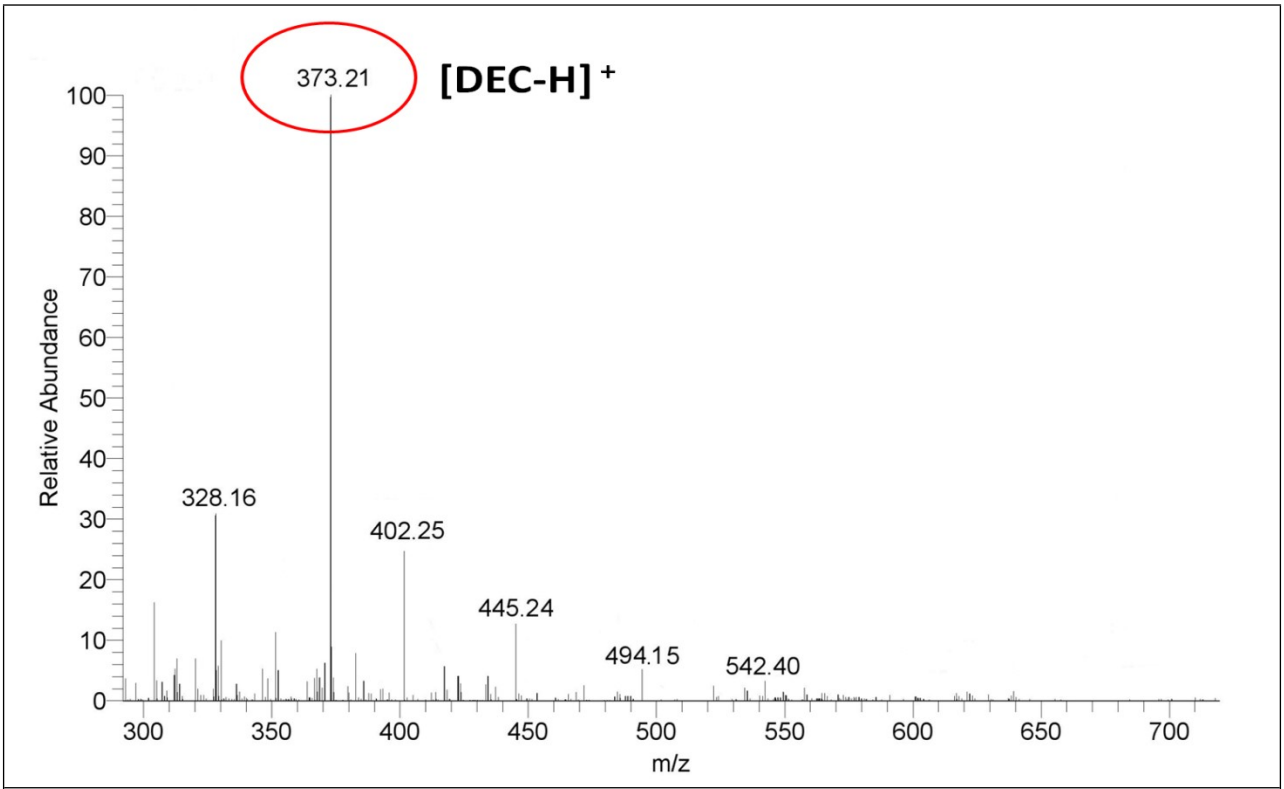

Figure S1a QTOF mass spectrum of **DEC**

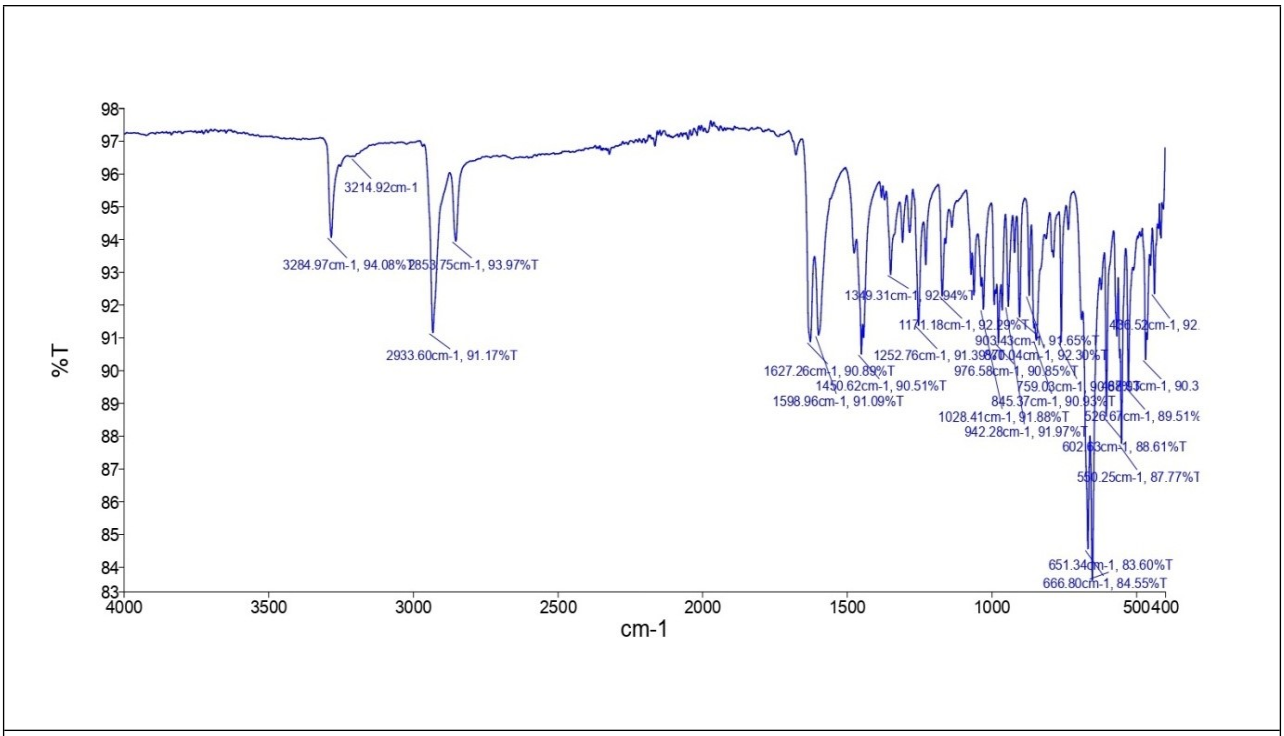

Figure S1b FTIR spectrum of **DEC**

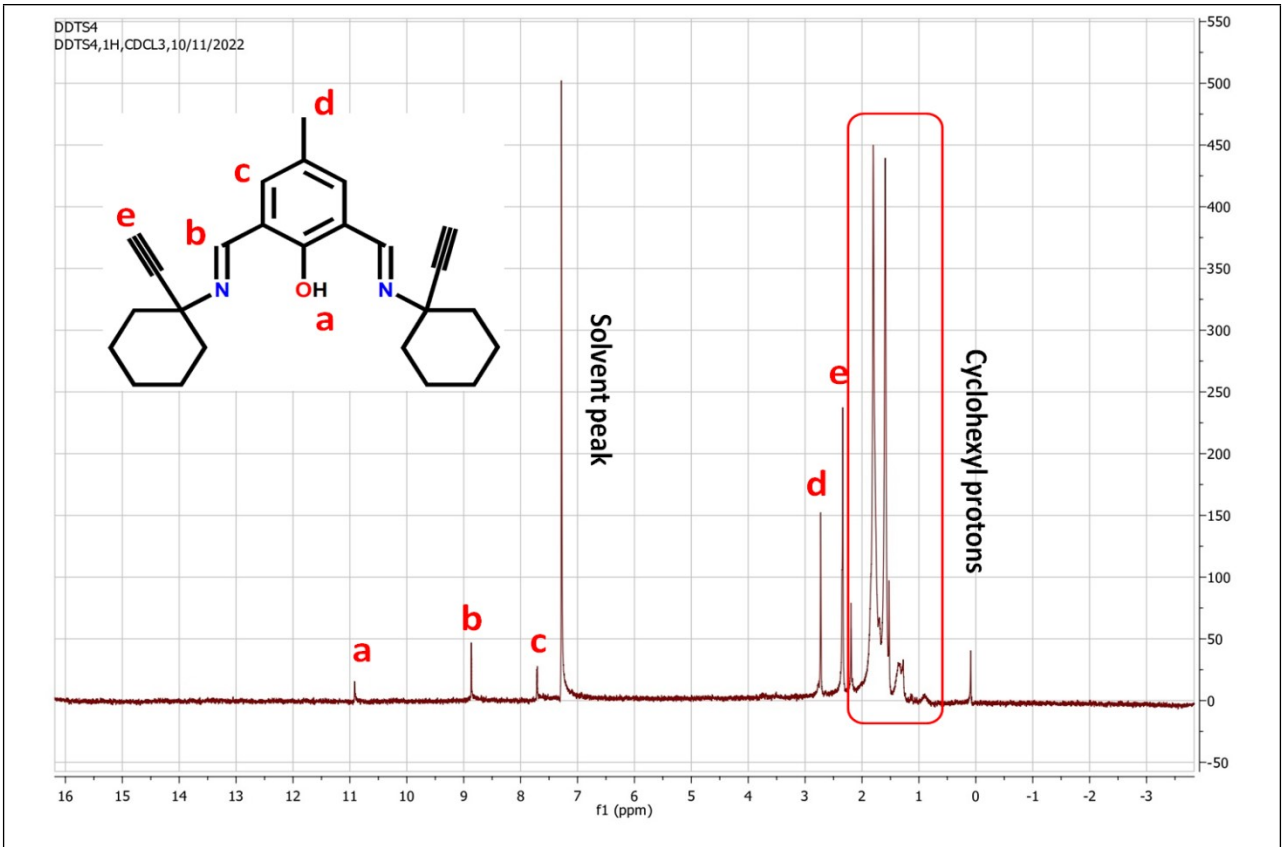

Figure S1c ^{1}H NMR spectrum of **DEC** in $CDCl_3$

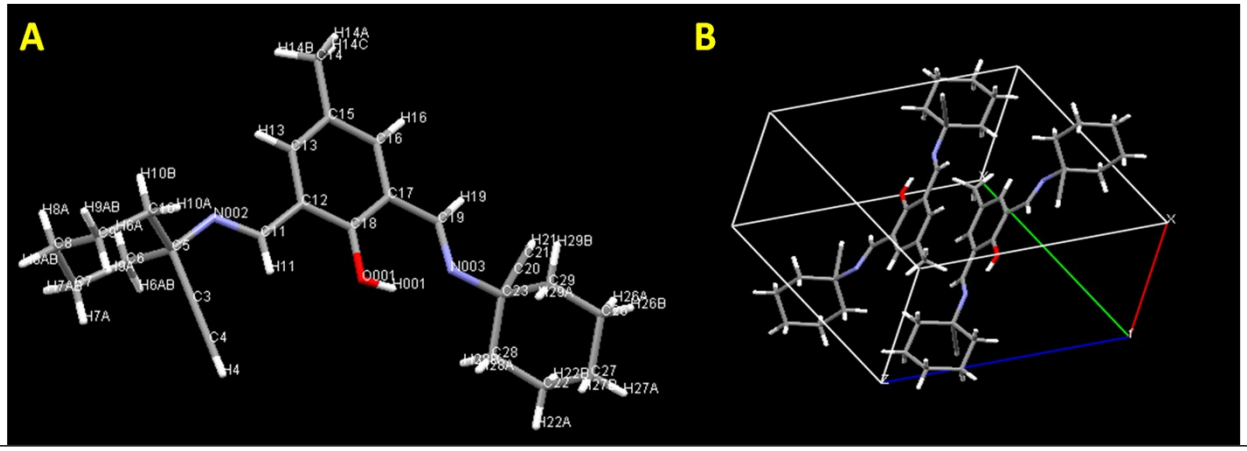

Figure S1d Single crystal X-ray structure of **DEC** with (A) atom labelling scheme and (B) packing diagram.

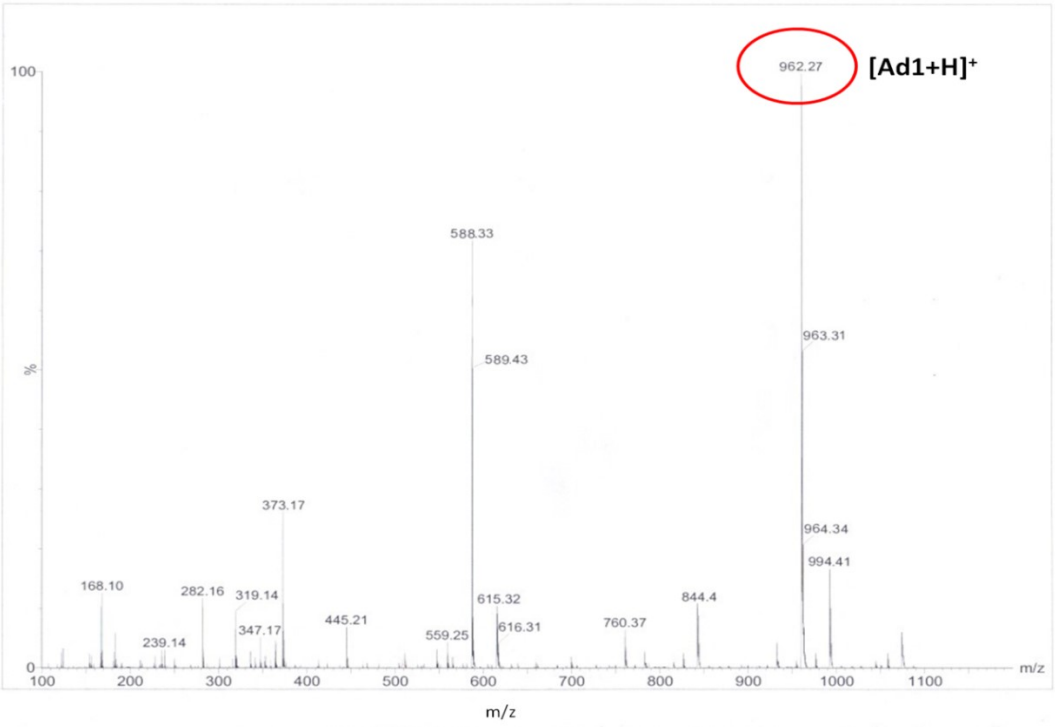

Figure S2a QTOF mass spectrum of **Ad1**

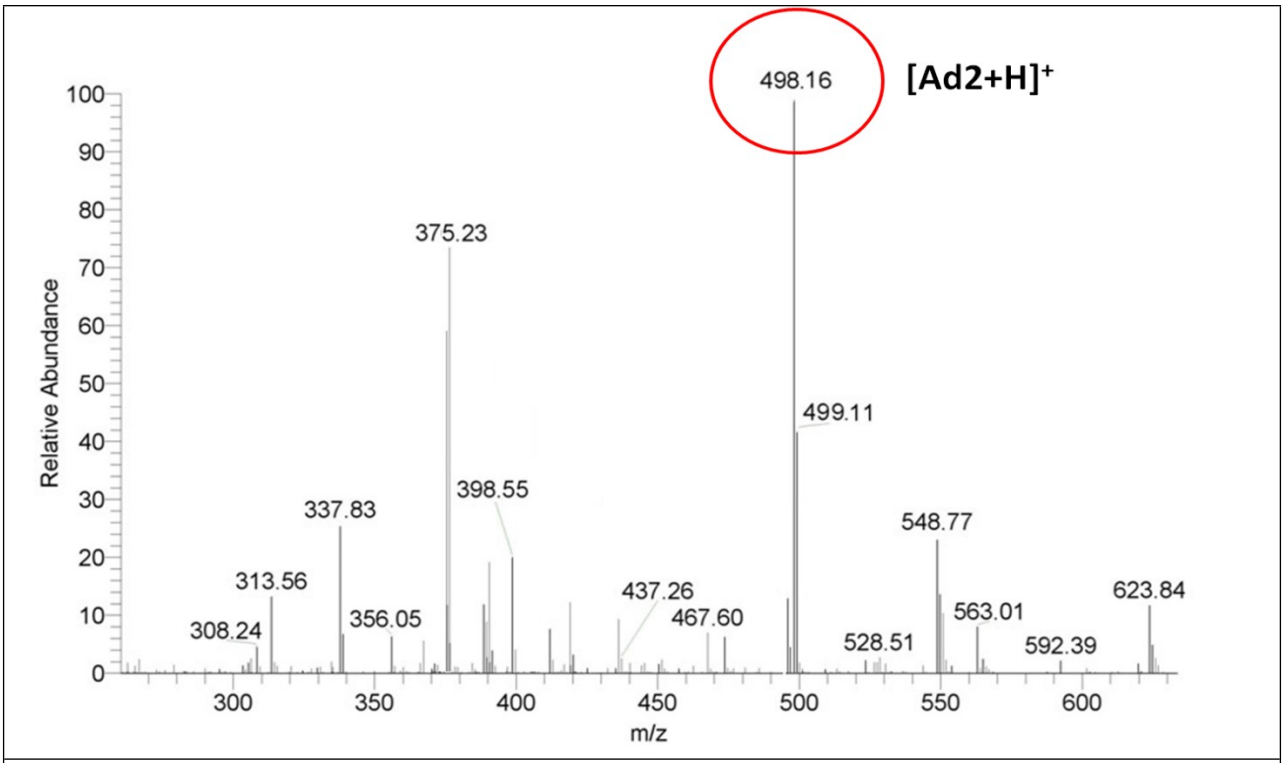

Figure S2b QTOF mass spectrum of **Ad2**

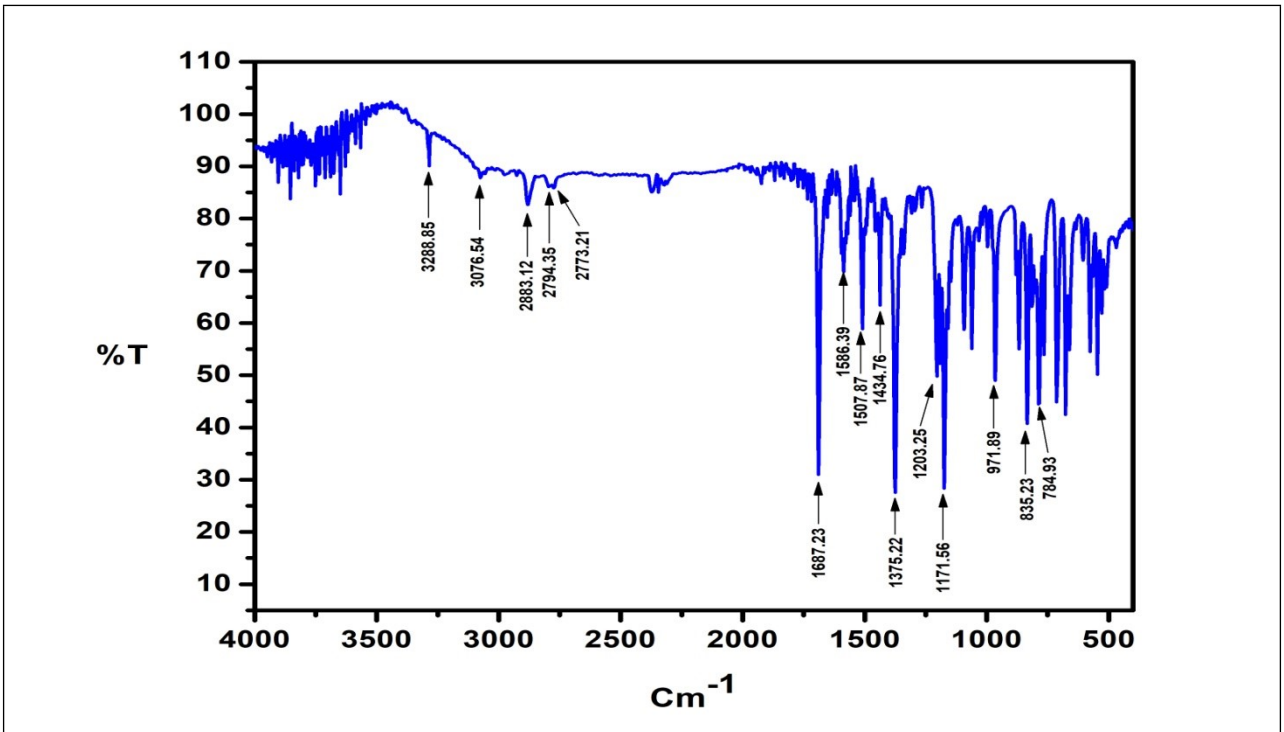

Figure S3a FTIR spectrum of **Ad1**

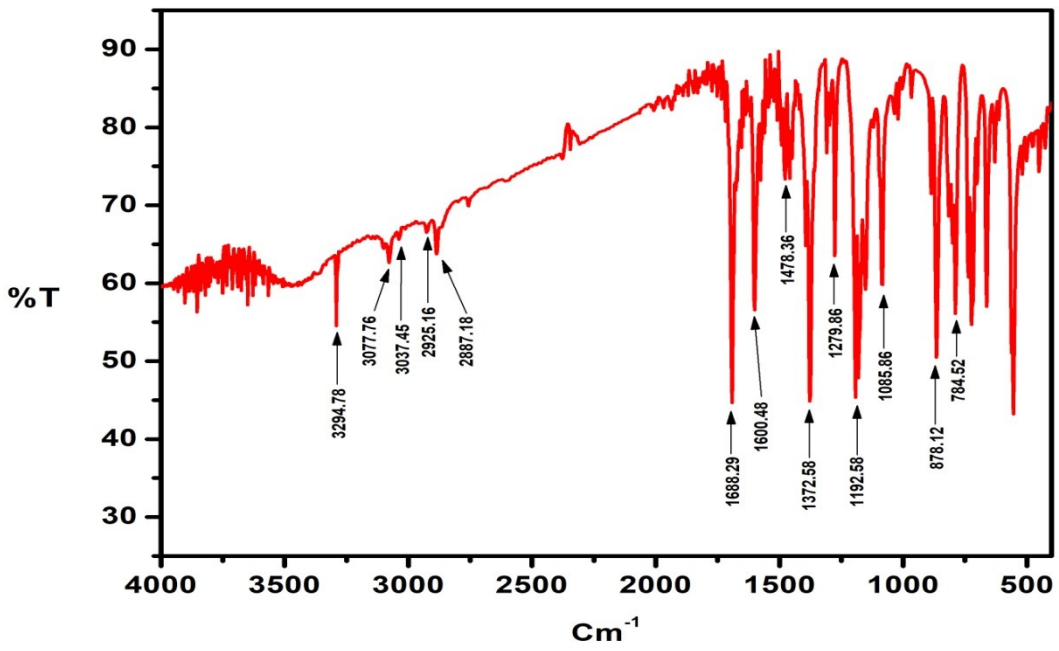

Figure S3b FTIR spectrum of **Ad2**

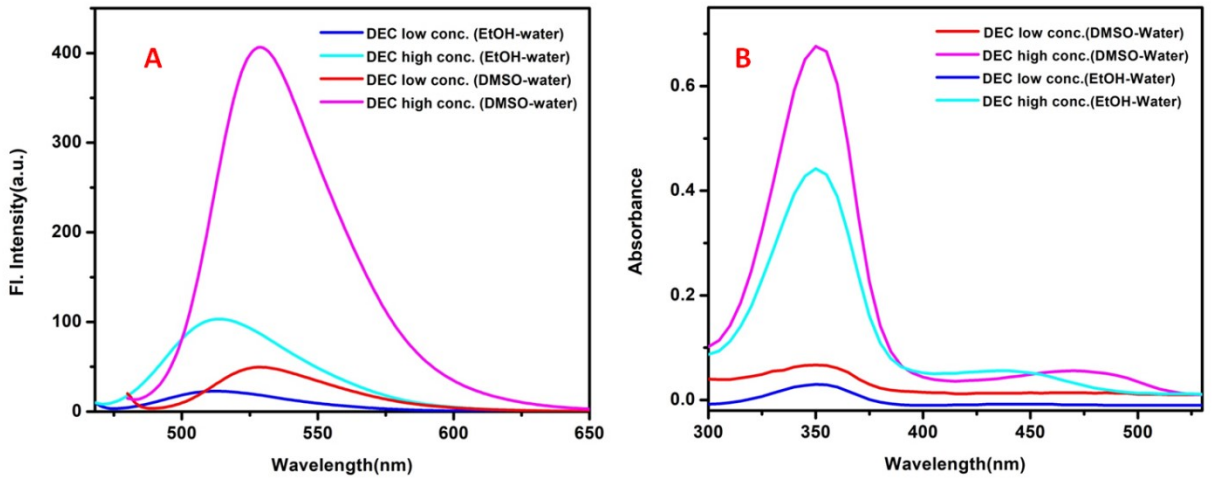

Figure S4 (A) Emission and (B) absorption spectra of DEC at different concentrations in DMSO-water and EtOH-water media.

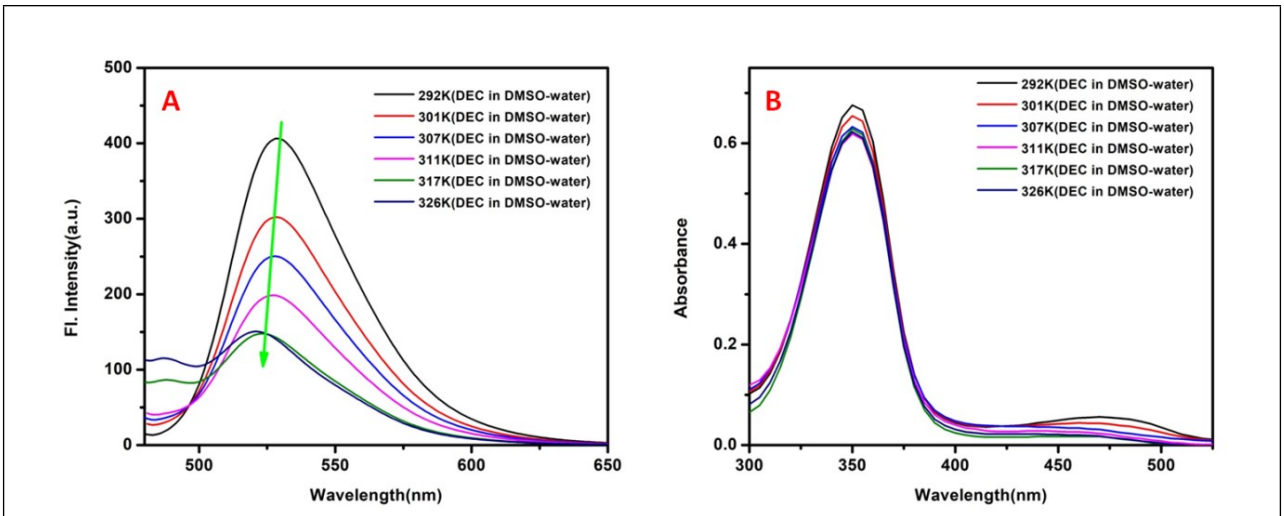

Figure S5a Emission (A) and absorption (B) spectra of **DEC** (150µM) in DMSO-water medium at different temperature.

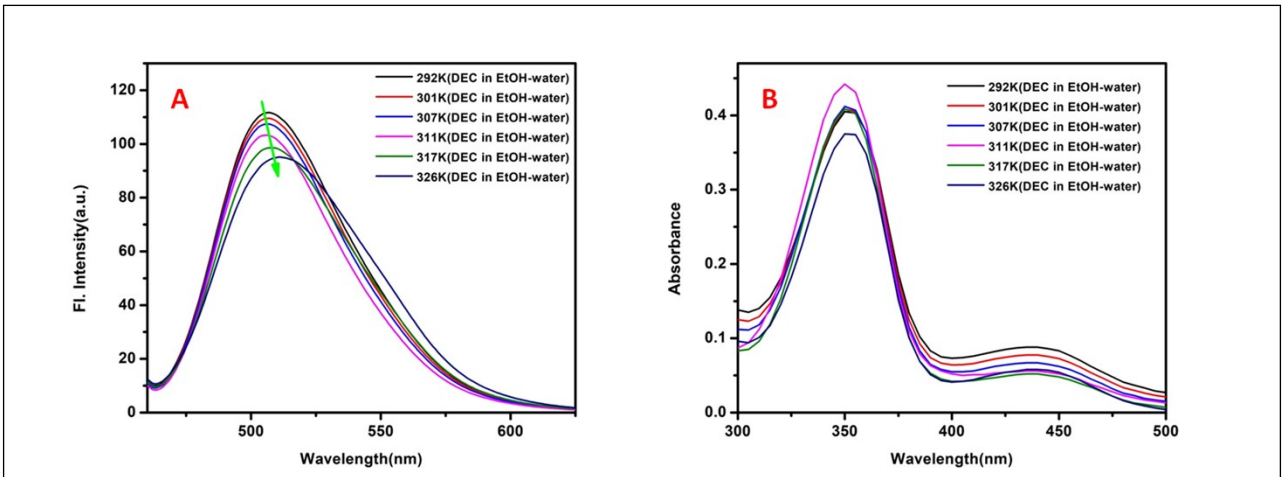

Figure S5b Emission (A) and absorption (B) spectra of **DEC** (150µM) in EtOH-water media at different temperature.

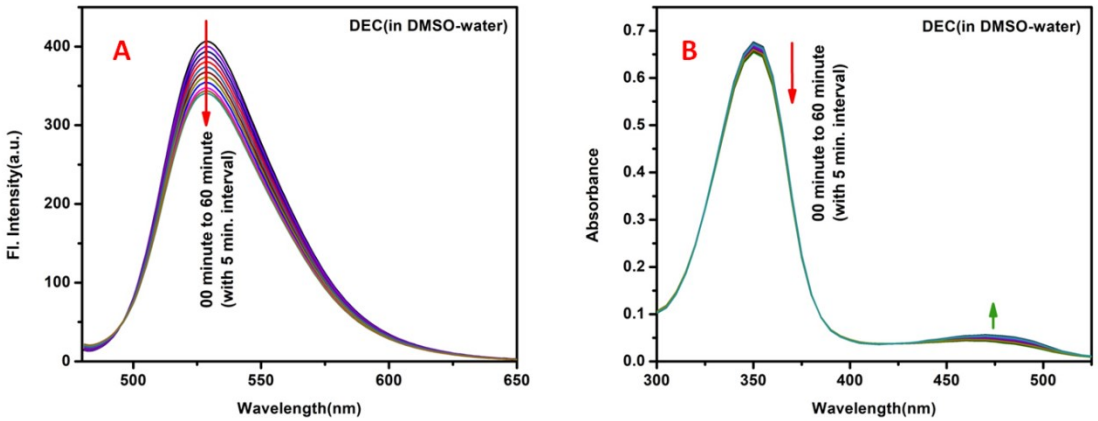

Figure S5c Variation of emission (A) and absorption (B) spectra of **DEC** (150 µM) in DMSO-water media upon exposure to sun light for different time span.

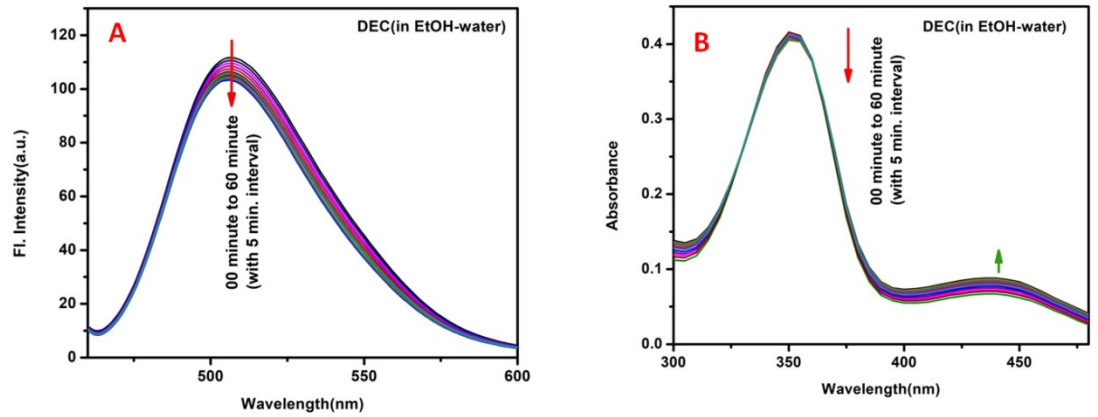

Figure S5d Variation of emission (A) and absorption (B) spectra of **DEC** (150µM) in EtOH-water media upon exposure to sun light for different time.

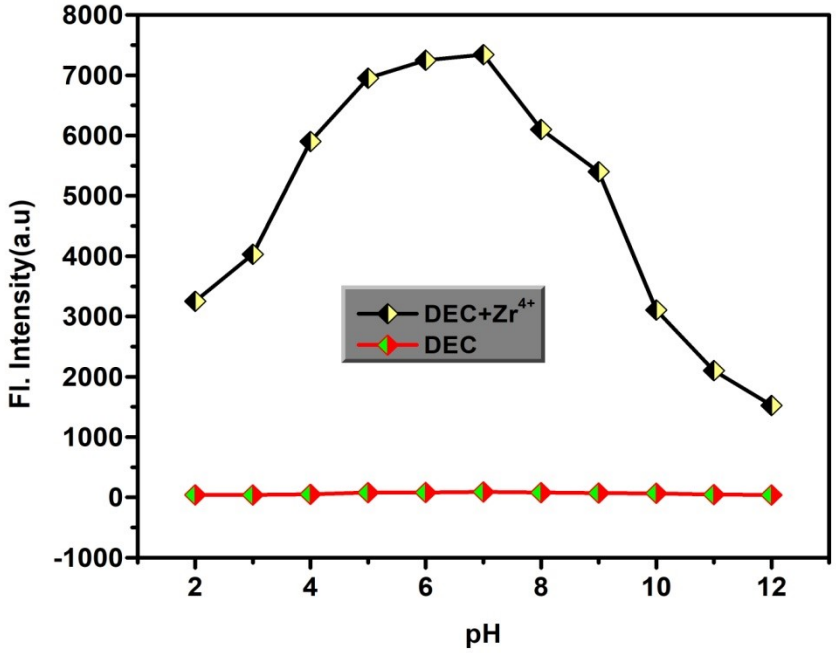

Figure S6 Effect of pH on the emission intensities of **DEC**(λ_{ex} = 380 nm, λ_{em} = 508 nm) in presence and absence of **Zr(IV)**

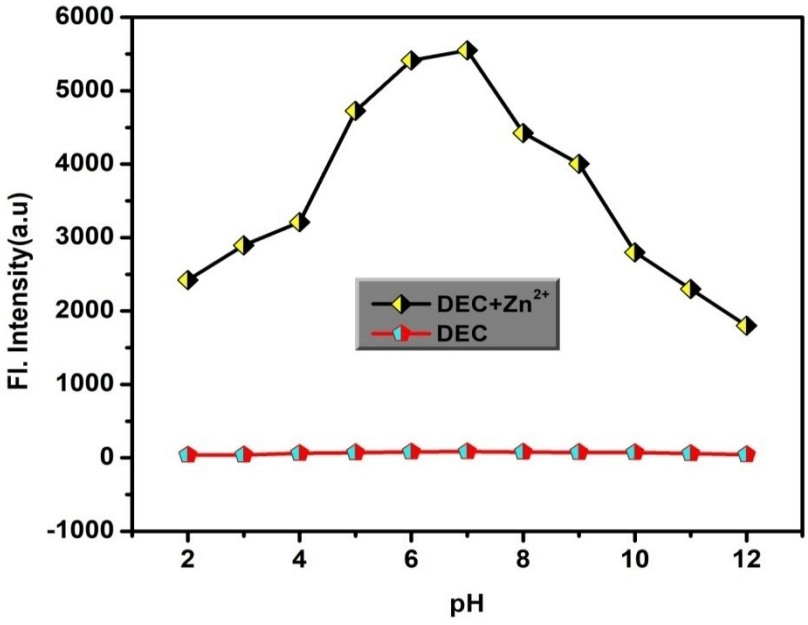

Figure S7 Effect of pH on the emission intensities of **DEC**(λ_{ex} = 350 nm λ_{em} = 474 nm) in presence and absence of **Zn(II)**

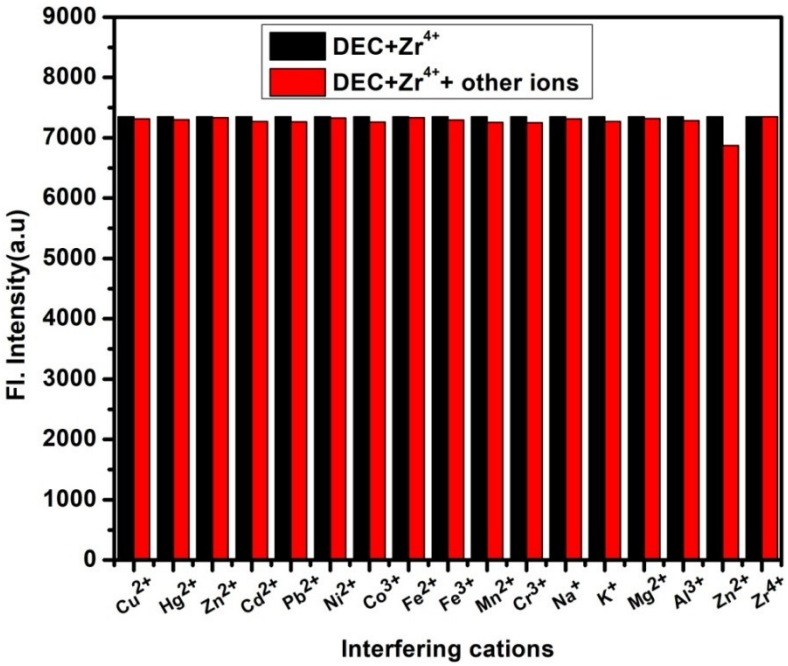

Figure S8 Interference studies for fluorescence detection of **Zr(IV)** using **DEC** (λ_{ex} = 380 nm, λ_{em} = 508 nm).

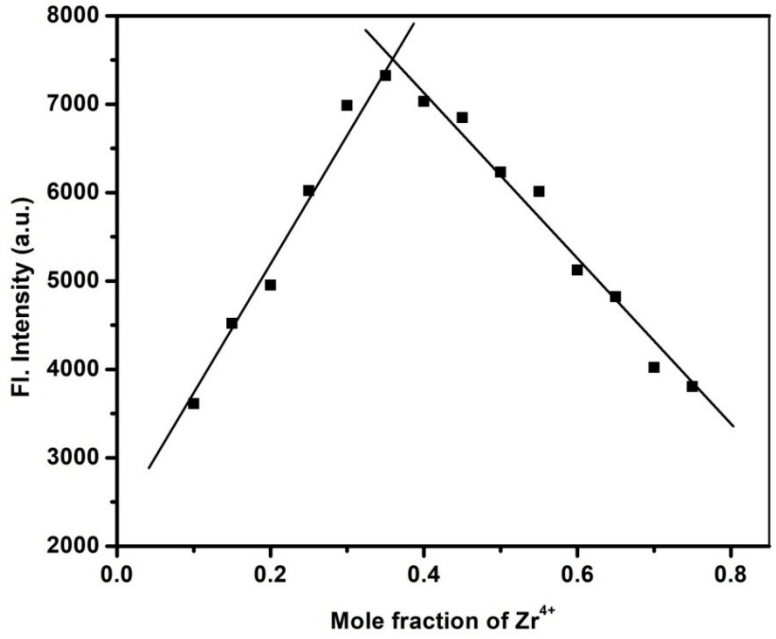

Figure S9 Job's plot for stoichiometry determination of [**DEC-Zr(IV)**] adduct (λ_{ex} = 380 nm, λ_{em} = 508 nm).

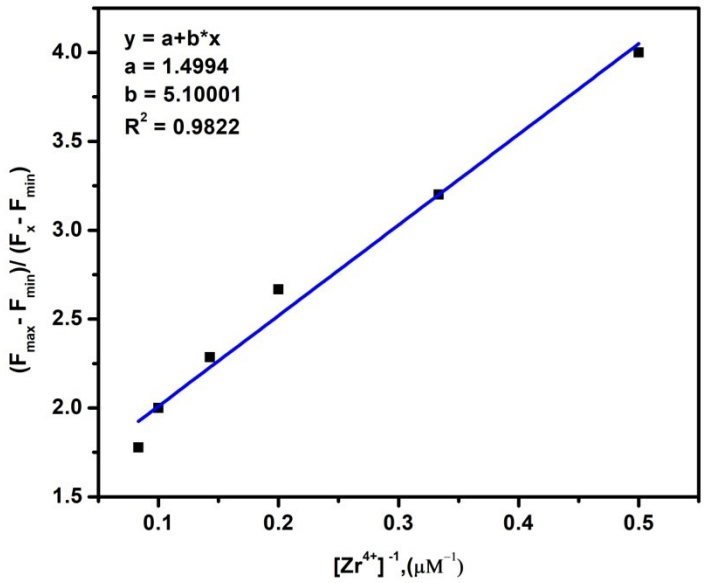

Figure S10 Benesi−Hildebrand plot for determination of association constant of **DEC** for **Zr(IV)** (liner portion) (λ_{ex} = 380 nm, λ_{em} = 508 nm)

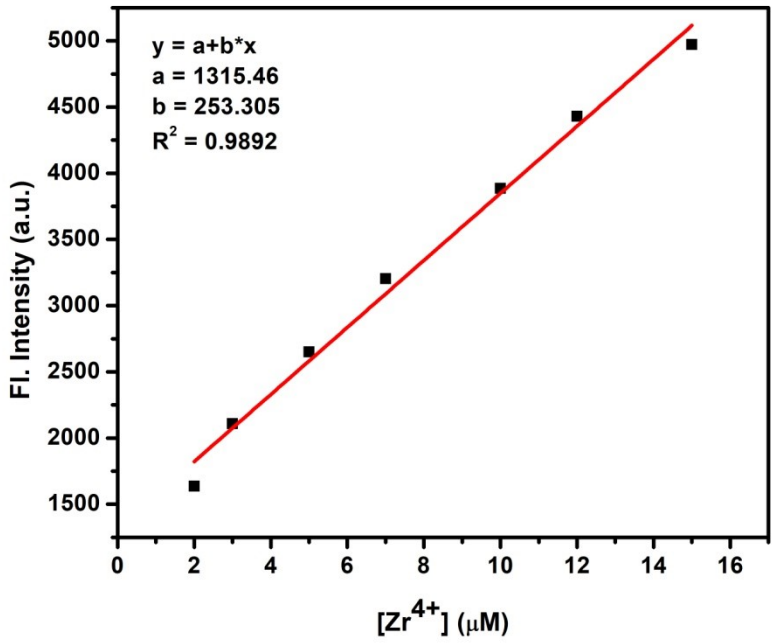

Figure S11 Determination of the detection limit based on change in the ratio (emission intensity) (λ_{ex} = 380 nm, λ_{em} = 508 nm) of **DEC** (40 μM) upon addition of **Zr(IV)**

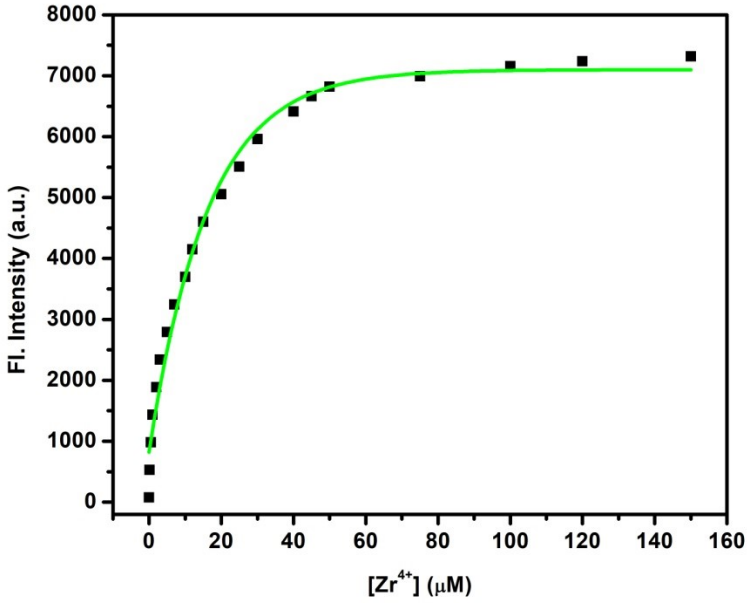

Figure S12 Plot of emission intensities of **DEC** (40 μM, λ_{ex} = 380 nm, λ_{em} = 580 nm) as a function of externally added **Zr(IV)** (1.0-160 μM)

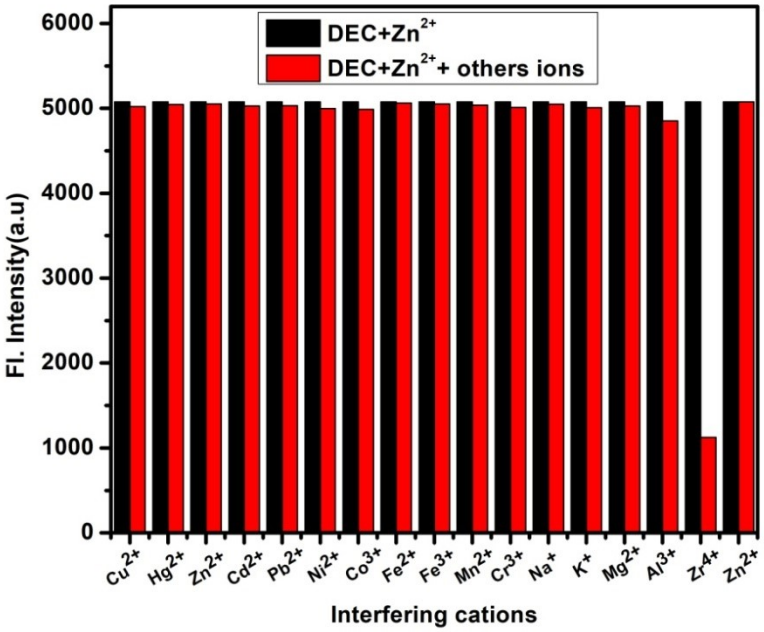

Figure S13 Interference studies for fluorescence detection of **Zn(II)** using **DEC** (λ_{ex} = 350 nm, λ_{em} = 474 nm).

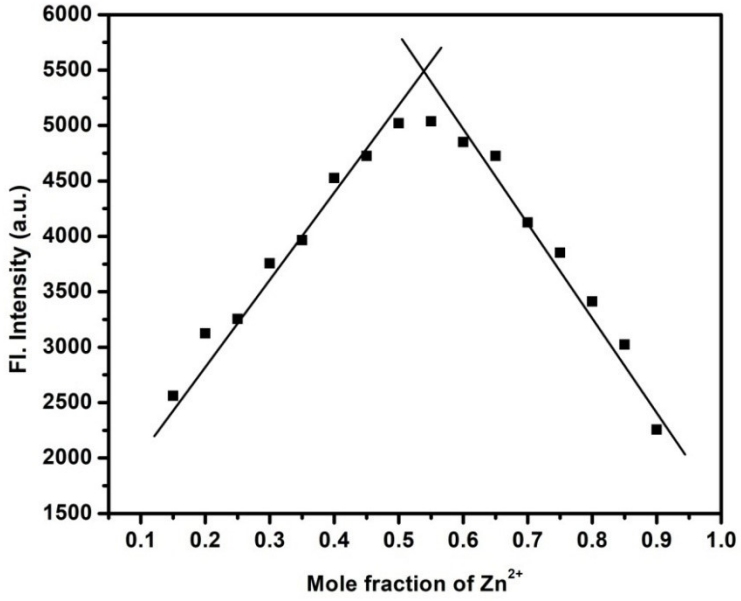

Figure S14 Job's plot for stoichiometry determination of [**DEC-Zn(II)**] adduct (λ_{ex} = 350 nm, λ_{em} = 474 nm).

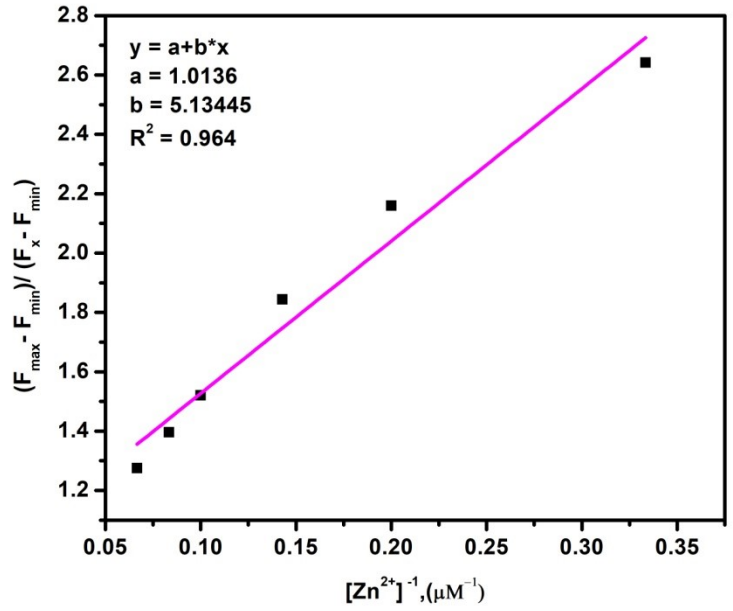

Figure S15 Benesi−Hildebrand plot for determination of association constant of **DEC** for **Zn(II)** (liner portion) (λ_{ex} = 350 nm, λ_{em} = 474 nm)

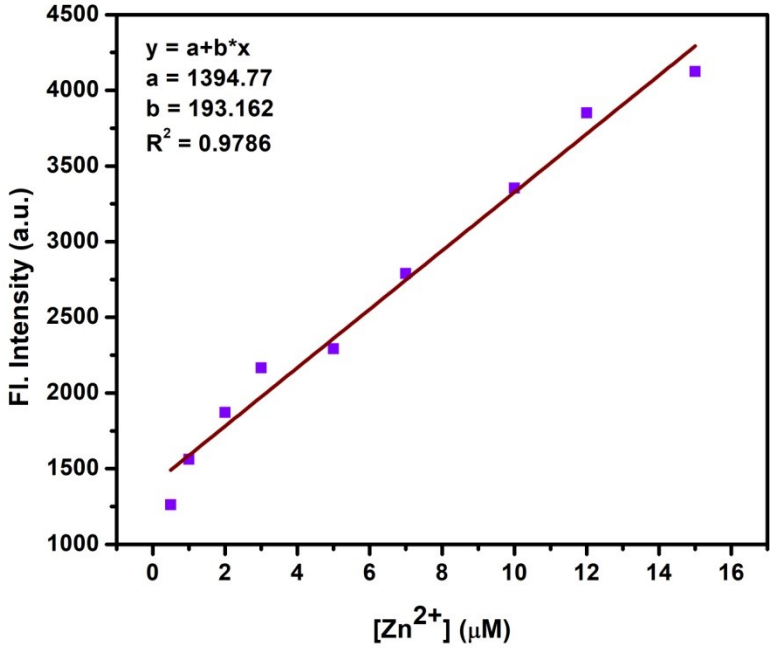

Figure S16 Determination of detection limit based on change in the ratio (emission intensity) (λ_{ex} = 350 nm, λ_{em} = 474 nm) of **DEC** (40 μM) upon addition of **Zn(II)**

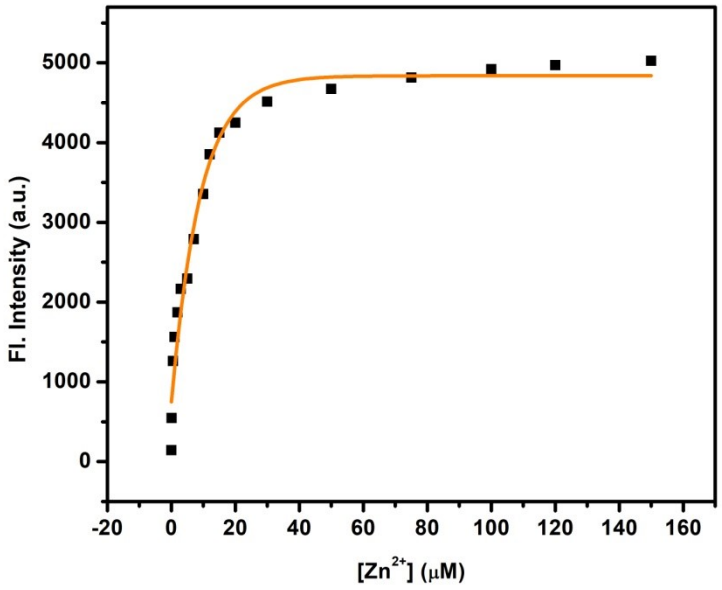

Figure S17 Plot of emission intensities of **DEC** (40 μM, λ_{ex} = 350 nm, λ_{em} = 474 nm) as a function of externally added **Zn(II)** (1.0-160 μM)

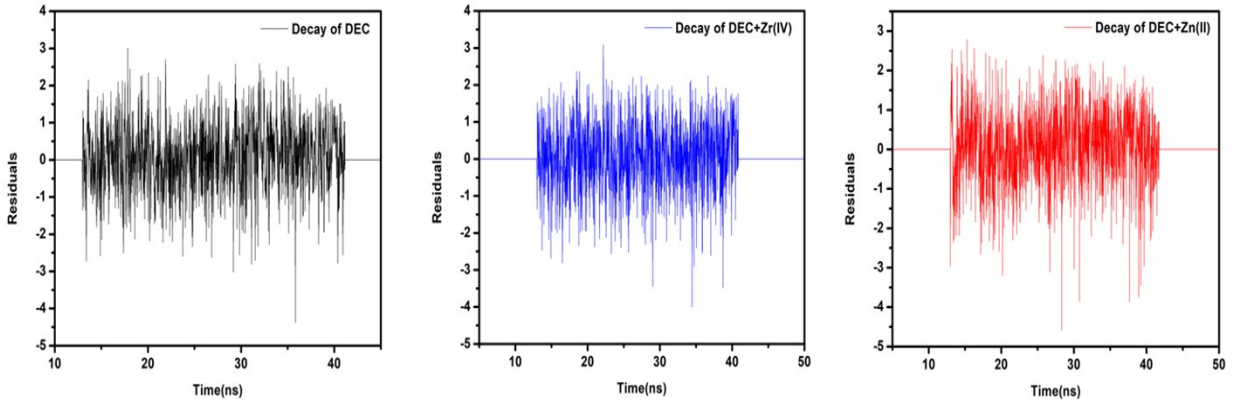

Figure S18 Residual plots for life time decay of DEC, [DEC- Zr(IV)] (**Ad1**) and [DEC- Zn(II)] (**Ad2**)